Received: 17 September 2020 | Revised: 11 March 2021 | Accepted: 17 June 2021

DOI: 10.1111/clr.13803

ORIGINAL ARTICLE

CLINICAL ORAL IMPLANTS RESEARCH WILEY

De novo bone formation around implants with a surface based on a monolayer of multi-phosphonate molecules. An experimental in vivo investigation

Javier Sanz-Esporrin[1,2] | Riccardo Di Raimondo[1] | Fabio Vignoletti[1] | Javier Núñez[1] | Fernando Muñoz[3] | Mariano Sanz[1,2]

[1]Postgraduate Section of Periodontology, Faculty of Odontology, University Complutense of Madrid, Madrid, Spain

[2]ETEP (Etiology and Therapy of Periodontal and Peri-implant Diseases) Research Group, University Complutense of Madrid, Madrid, Spain

[3]Ibonelab, Department of Veterinary Clinical Sciences, University of Santiago de Compostela, Lugo, Spain

Correspondence
Javier Sanz-Esporrin, Faculty of Odontology, Universidad Complutense de Madrid, Plaza Ramon y Cajal s/n, 28040 Madrid, Spain.
Email: javier.sanz.esporrin@ucm.es

Funding information
This study was partially funded through a research contract between the University Complutense of Madrid and MIS Implants (Israel)

Abstract

Objectives: The purpose of this experimental in vivo investigation was to evaluate the influence of modifying the implant surface by adding a monolayer of multi-phosphonate molecules on the *de novo* bone formation and osseointegration.

Material and Methods: The study was designed as an animal preclinical trial with intra-animal control and two healing periods, 2 and 8 weeks, to compare implants with an identical macro-design but with two different surfaces. Eight female Beagle dogs participated in the study. Control implants had a moderately rough surface combining sandblasting and acid etching; test implants had an additional monophosphonate layer covalently bonded to titanium. Histologic and radiographic (micro-CT) outcome variables were evaluated.

Results: The first bone-to-implant contact (fBIC) was located more coronally for the test implants at the first (0.065 mm (95% CI = −0.82, 0.60)) and second healing milestones (0.17 mm (95% CI = −0.9, 0.55)). Most coronal BIC of the test implants displayed a higher percentage of osseointegration, +6.33% and +13.38% after 2 and 8 weeks, respectively; however, the differences were not statistically significant. The micro-CT examination did not show any BIC difference.

Conclusions: The monophosphonate layer coating demonstrated clinical, histological, and radiographic results similar to the control surface.

KEYWORDS

animal model, dental implants, histology, implant surface, osseointegration, monophosphonate layer, wound chamber, histometric analysis, micro-CT

Supporting Information: ARRIVE guidelines checklist.

1 | INTRODUCTION

Since the first description of the osseointegration phenomenon (Albrektsson et al., 1981; Branemark et al., 1969, 1977), the healing of dental implants placed in alveolar bone has been extensively studied providing clear histological documentation on the biological cascade of events that guides bone and soft tissue healing around dental implants (Berglundh et al., ,2003, 2007). Surface treatment modifications have been a field of great research interest seeking to improve the dynamics of osseointegration and the quality and quantity of bone-to-implant contact (Junker et al., 2009). An increase in surface roughness was the first modification that demonstrated an increase in bone apposition (Abrahamsson et al., 2004; Buser et al., 1991; Wennerberg et al., 1995), and a reduced non-loading time between implant placement and prosthetic restoration (Lazzara et al., 1998). In fact, significantly higher success and survival rates were reported when moderately rough surfaces were compared with machined surfaces (Cochran, 1999). Other modifications have included different surface coatings, such as hydroxyapatite coatings, but the latter may be infected and lead to unwanted tissue reactions (Abrahamsson et al., 2013; Albrektsson et al., 2008; van Oirschot et al., 2013; Wheeler, 1996). Research efforts have evolved toward modifying the chemical structure of titanium by incorporating fluoride ions (Ellingsen et al., 2004) or by augmenting the surface wettability when implants are maintained submerged in an isotonic NaCl solution (Buser et al., 2004). Another chemical surface treatment modification has been the application of a covalently bonded layer of monophosphonate molecules on titanium. The presence of Ti-O-P bound is clearly depicted by XPS analysis demonstrating a strong covalent bound that provides stability, thus producing an ultrathin layer that covers the microtextured surface, which prevents the peeling off the underground surface, as it happens with conventional thick coatings. The aim of this surface treatment was to attract and stimulate bone-forming cells, thus providing this surface with osteoconductive properties. This effect has been demonstrated in vitro (Viornery et al., 2002) but has not been tested in oral environment in preclinical experimental studies. It was, therefore, the purpose of this experimental in vivo investigation was to study the histological and radiographic response of *de novo* bone formation on this novel implant surface compared with implants with identical macro-design but without this very surface chemical modification.

2 | MATERIAL AND METHODS

2.1 | Study design and randomization

The study was designed as a preclinical trial with two-time healing periods (2 and 8 weeks after implant placement) comparing two implants with identical macro-design but different surface characteristics. Beagle dog was chosen as experimental model. The study protocol consisted on four interventions: (i) tooth extraction, (ii) implant placement (healing T8), (iii) implant placement (healing T2), and (iv) euthanasia and subsequent histological processing and evaluation. The experimental sites were randomly allocated to either test or control according to a computer-generated randomization list (IBM SPSS Statistics® V20. JM. Domenech). Randomization sequence was generated using a blocking, balanced restricted randomization, stratified by hemimandible and implant position (P1-P5). Furthermore, each hemimandible (left or right) randomly allocated one healing time point (T2 or T8). Allocation to the treatment was concealed by means of sealed envelopes containing the implant type, which were opened during the surgical procedure once the flaps were raised and the bone was exposed.

2.2 | Experimental sample

A total of eight healthy adult female Beagle one-year-old dogs (mean weight 14.63 kg) (Isoquimen, Barcelona, Spain) were used in this experimental in vivo investigation, in full compliance with the ARRIVE guidelines.

The Ethical Committee of the Jesús Usón Minimally Invasive Surgical Center (Cáceres, Spain) approved the study protocol (ES register number: 201520930011504). The animals were housed in the Animal experimentation Service Facility of the Jesús Usón Minimally Invasive Surgical Center (Cáceres, Spain), and the surgeries were carried out in the same premises from January 2016 to May 2016. All the experiments were performed according to the Spanish and European regulations about care and use of research animals; the dogs were monitored daily during the study by a veterinarian accredited in laboratory animal science. According with animal welfare, vaccine and antiparasitic drugs were administrated upon arrival; they were then identified with a microchip and housed in pairs. Animal housing conditions were room temperature between 18 and 29°C, 30%–70% of relative humidity, and 15 min air renewal per hour. A 12 hr light/dark cycle with intensity control was established; feeding and water intake was evaluated daily. The experimental segment of the study started after an adaptation/quarantine period of 3 weeks.

2.3 | Study devices

Implants were MIS® C1 implants (MIS implants technologies LTD, Israel), with 3.5 mm of diameter and 9 mm of length. All implants presented a moderately rough surface with and S_a of 1.22 ± 0.09. Implants presented the same macroscopic design (Figure 1h), which included a customized modification by creating a 0.40-mm deep U-shaped circumferential trough within the thread region (intraosseous portion), although leaving the tip of each thread untouched (Figure 1i). In this manner, an experimental wound chamber was created following implant installation to allow for a validated study of the bone healing and osseointegration after implant placement (Abrahamsson et al., 2004; Berglundh et al., 2003).

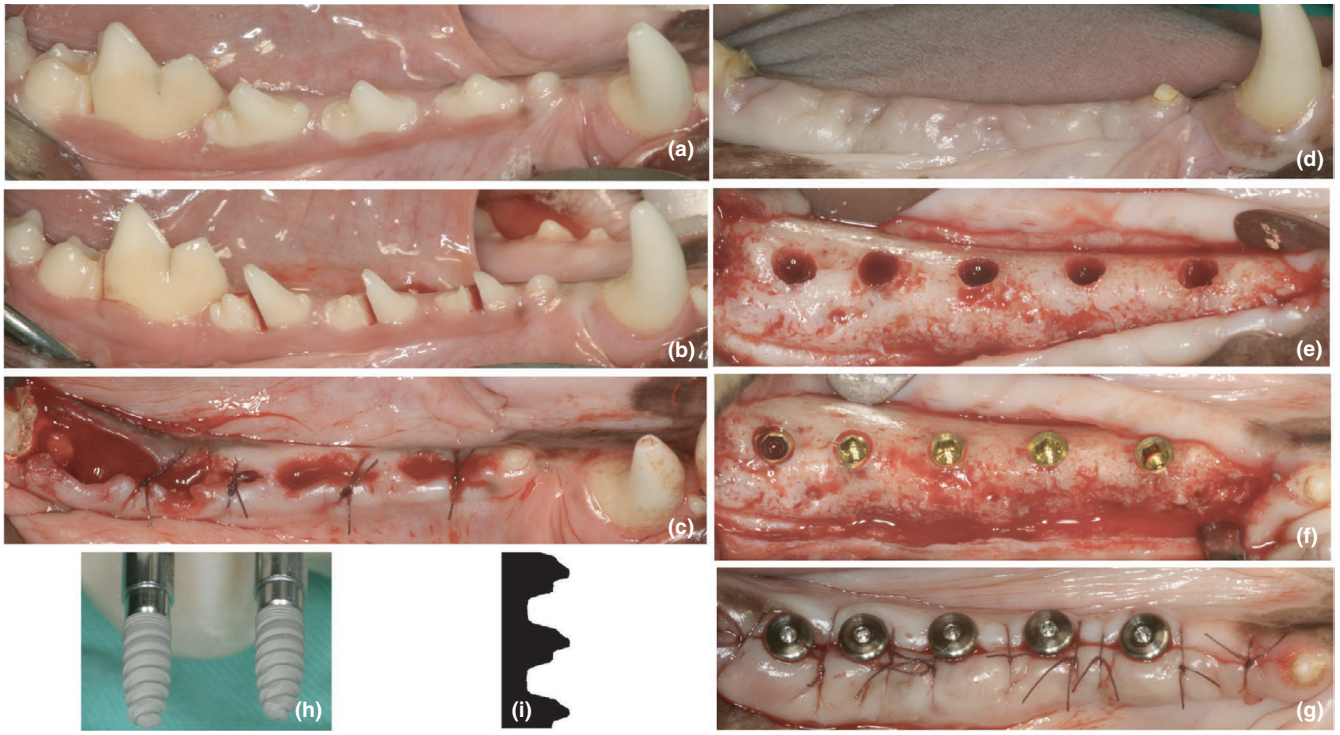

FIGURE 1 Clinical stages of the experiment. (a) Baseline situation. (b) Teeth hemi-section prior to extraction. (c) Suture after teeth extraction. (d) Healed crest 3 months after extractions. (e) Implant osteotomies. (f) Implant placement. (g) Suture after implant placement. (h) Identical macroscopic design of test and control implants. (i) Wound chamber thread design; increased 0.40-mm deep U-shaped valley between threads to allow bone healing study

The surface of test implants included a covalently bonded phosphonate treatment that created a nanometer thin molecular nanolayer of monophosphonate molecules, also known as phosphonic acids (Nano Bridging Molecules, Gland, Switzerland), without altering the geometry and roughness of the implant surface. Unlike phosphates, phosphonic acids (phosphonates) are a family of organophosphorus compounds, which make them able to react and connect to the titanium oxide surface. The control surface presented the conventional moderately rough MIS implant surface based on sandblasting and etching, without the monophosphonate chemical treatment. Both test and control implants presented the same roughness (moderately rough–Sa 1.22 ± 0.09). Fabrication process of the test implant surface treatment is protected by the patent (EP1698357), which is commercially available under the product name MIS B+® (MIS implants technologies LTD, Israel).

In total, 40 tests and 40 control implants were placed. From those, 20 test and 20 control implants were placed in the 2-week healing group hemimandibles and 20 test and 20 control implants were placed in the 8-week healing group hemimandibles. In each hemimandible, both test and control implants were placed according to random allocation in the corresponding healing period.

2.4 | Surgical procedures

All surgical interventions were performed under sterile conditions, in an animal operating theater and under general anesthesia induced by Propofol (3–5 mg/kg/i.v., Propovet®, Abbott Laboratories, Kent, UK) and maintained on a concentration of 2.5%–4% of isoflurane (Isobavet®, Schering-Plough, Madrid, Spain). The animals were first premedicated with medetomidine (20 μg/kg/i.m., Domtor, Esteve, Barcelona, Spain) and the pain controlled with the administration of morphine (0.4 mg/kg/i.m., Morfina Braun 2%, B. Braun Medical, Barcelona, Spain). During anesthesia, the animals were continuously monitored by a veterinarian category B or C, controlling electrocardiography, capnography, pulsioxymetry, and non-invasive blood pressure. Prophylactic administration of Cephazolin (20 mg/kg/i.v., Kurgan, Normon, Madrid, Spain) and Cefovezin (8 mg kg^{-1} s^{-1}.i.d./s.c., Convenia, Zoetis, Madrid, Spain) was performed intraoperatively. At the end of the procedures, Atipamezole (50 mg/kg/i.m., Esteve, Barcelona, Spain) was administered to revert the effects of Medetomidine. Postoperative pain was controlled by administration of morphine (0.2 mg/kg/i.m./6 hr, Morfina Braun 2% B. Braun Medical, Barcelona, Spain) and meloxicam as anti-inflammatory and analgesic treatment (0.2 mg/kg/i.m./SID, Metacam, Boehringer Ingelheim, Barcelona, Spain) for 5 days.

The surgical protocol used in this study has been was recently reported in detail in another publication from our research group (Vignoletti et al., 2019). In brief:

2.4.1 | Phase 1: tooth extraction

Extraction of mandibular 2P2, 3P3, 4P4 premolars, and the mesial root of 1M1 was carried out in both jaws, once teeth were hemisected using a flapless procedure. (Figure 1a–c).

2.4.2 | Phase 2: implant placement (8-week healing group)

Full-thickness buccal and lingual flaps were elevated from distal of the cuspid to distal of M1 and 3 mm of the alveolar ridge was exposed. Once the appropriate osteotomies were done and after randomization and implant allocation, implants were inserted following the standard manufacturing instructions. Implants were placed at the level of the crest (bone level), taking as reference buccal plate. In some of the cases, lingual aspect of the implant remained subcrestally located, as the crest presented irregular shape with a more apical buccal bone place with respect to the lingual plate. Healing abutments were secured, and flaps were sutured to allow for transmucosal healing. A total of five implants were placed in each hemimandible following randomization. (Figure 1d–g). Postoperatively, the animals had professional plaque control consisting the application of gauzes embedded in chlorhexidine solution 0.12% (Perio-Aid Treatment®, Dentaid, Cerdanyola del Valles, Spain) three times a week during the first two weeks and then 3 times a week with toothbrush and chlorhexidine gel. Surgeries were performed in one randomized (left or right) hemimandible of each dog, leaving the contralateral hemimandible for the 2-week healing group). Each hemimandible harbored both, test and control implants, allocated in a randomized sequence.

2.4.3 | Phase 3: implant placement (2-week healing group)

Two weeks prior to euthanasia, the same surgical procedure and postoperative protocol were performed in the contralateral corresponding hemimandible according to the randomization sequence.

In total, 40 tests and 40 control implants were placed, 20 test and 20 control implants in the 2-week healing group and 20 test and 20 control implants in the 8-week healing group.

2.4.4 | Phase 4: euthanasia

After 2 weeks of healing, dogs were first sedated with medetomidine (30 μg/kg/i.m., Esteve, Barcelona, Spain) and then euthanized with an intravenous overdose of sodium pentobarbital (40–60 mg/kg/i.v., Dolethal, Vetoquinol, France). Subsequently, the lower jaws were dissected and retrieved with intact soft tissues and fixed in buffered 10% formaldehyde solution. Previous to histological processing, the implants were individually separated using a band saw for micro-CT scanning.

2.5 | Micro-CT analysis

All specimens were scanned before being sectioned using a high-resolution micro-CT (Skyscan 1,172, Bruker micro-CT NV, Kontich, Belgium). The X-ray source was set at 100 Kv and 100 μA with a voxel size of 12 μm and an Aluminum/Copper filter (Al/Cu). Scanning was performed over a 360° rotation acquiring images every 0.4°. Once scanned, the images were reconstructed based on the Feldkamp algorithm using the NRecon software (Bruker micro-CT NV, Kontig, Belgium). The reconstructed images were evaluated with the Data Viewer software (Bruker micro-CT NV, Kontig, Belgium) and rotated to ensure that the implant was perfectly aligned. A VOI of 4 mm of length was selected in the middle of the implant for all the samples, including all the surrounding bone in the four directions (distal, mesial, buccal, and lingual).

After selecting the volume of interest (VOI), data were analyzed using the CTAn software (Bruker micro-CT NV, Kontig, Belgium). Firstly, a circular VOI of 5 mm of diameter was selected. Then, images were segmented using adaptative local thresholding methods, selecting the best threshold parameters for bone and for implant. The following outcomes were measured: (a) bone-to-implant contact (BIC; %) expressed as 360° bone-to-implant contact (intersecting bone), (b) implant volume and bone volume (%) using the method described by Bruker in the method note (074) "Osteointegration: analysis of bone around a metal implant" (January 2015), expressed as Bone volume/Tissue volume. (Figures 2 and 3).

2.6 | Histological processing

Using a randomization protocol, half of the blocks containing the implant and the surrounding hard and soft tissues were dissected and processed for ground sectioning following the method described by Donath and Breuner (Donath & Breuner, 1982). The samples were dehydrated in a graded series of ethanol solutions and embedded in a light-curing resin (Technovit 7,200 VLC; Heraeus-Kulzer GMBH, Werheim, Germany). To assure sectioning the implants in the longitudinal axis, the resin blocks containing the implants and adjacent tissues were radiographed in a buccal-lingual direction and using a ruler and a negatoscope, pencil lines were traced over the surface of the block to guide the sectioning of the block with a bandsaw equipped with a laser-aided orientation device (Exakt Apparatebau, Norderstedt, Germany). After sectioning, polishing was performed mechanically using 1,200 and 4,000 grit silicon carbide papers (Struers, Copenhagen, Denmark). Finally, the blocks attained a final tissue thickness of about 30 μm. The slides were stained according to the Levai Laczkó method (Jeno & Geza, 1975).

The second half of the specimens were prepared for decalcification following the "fracture technique" protocol described by Berglundh et al. (Berglundh et al., 1994).

2.7 | Histomorphometric analysis

The histometric evaluation was carried out using a Nikon Eclipse Ti microscope (Nikon, Heidelberg, Germany) equipped with image analysis software (Q-500MC; Nikon). One buccolingual section per

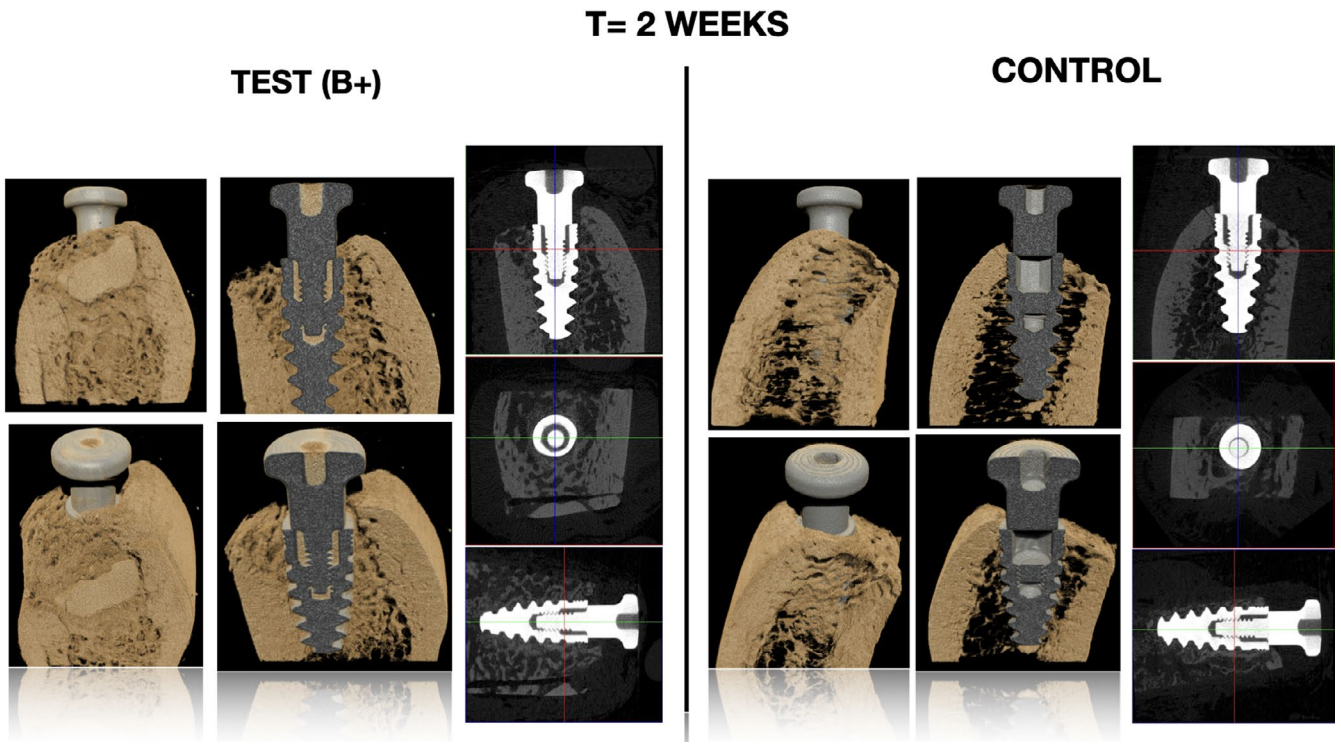

FIGURE 2 Two weeks healing micro-CT volumetric reconstructions

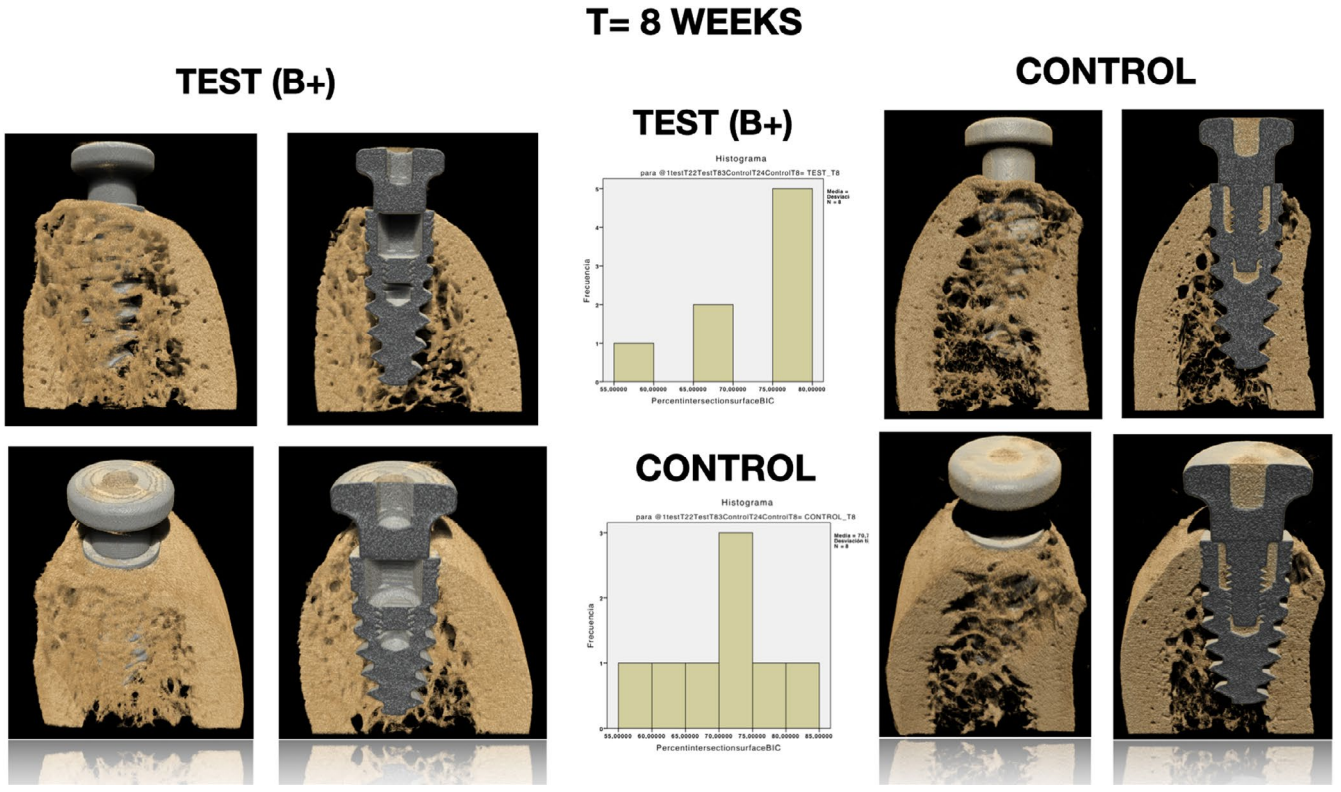

FIGURE 3 Eight weeks healing micro-CT volumetric reconstruction and frequency distribution histogram of results

implant was analyzed. All measurements were evaluated by two calibrated investigators masked to the specific experimental conditions (JS and RDR). The calibration test consisted on repeated evaluation of the bone-to-implant contact over the first section of each animal. Resulting inter-examiner intraclass correlation coefficient was 0.988 (95% confidence intervals: 0.982–0.999); intra-examiner intraclass

correlation coefficients were 0.999 (95% confidence intervals: 0.998–1.000) for JS and 1.000 (95% confidence intervals: 0.999–1.000) for RDR.

The following landmarks were identified on both the buccal and lingual sides in each implant (Figure 4):

- Implant shoulder (I),
- The first coronal level of bone in contact with the implant (B),
- Bone crest, defined as the most coronal point of bone (Bc).

Using these landmarks, the following linear measurements were calculated in millimeters at both the buccal and lingual aspects:

- I-Bc
- I-B
- Bc-B

The percentage of bone-to-implant contact (BIC) was calculated along a selected surface on the buccal and lingual aspects of test and control implants. BIC was evaluated at the most coronal portion (3 mm) as well as on the entire surface (6 coronal mm) of the implant (Figure 5).

The area of the wound chamber was selected (Figure 6), and percentages of each tissue component were calculated considering the total wound chamber area as 100%. The areas of newly formed bone and parent bone were measured within the wound chamber. Three wound chambers (buccal and lingual) were analyzed for each implant (Abrahamsson et al., 2004; Berglundh et al., 2003).

2.8 | Statistical analysis

Data from both histological and micro-CT analysis were expressed in means (±*SD*), considering the dog as the statistical unit of analysis ($n = 8$). The data were tested for normality by means of a Shapiro–Wilk test. Comparisons between experimental/control implants and between 2- and 8-week healing periods were analyzed using the two-way ANOVA and compared using generalized estimation model with intragroup comparisons. Bonferroni post hoc analysis was further performed to evaluate differences between the time intervals. Differences were considered statistically significant when p was <.05. This statistical analysis was performed using the software SPSS (SPSS® 20.0, SPSS Inc., Chicago, IL, USA).

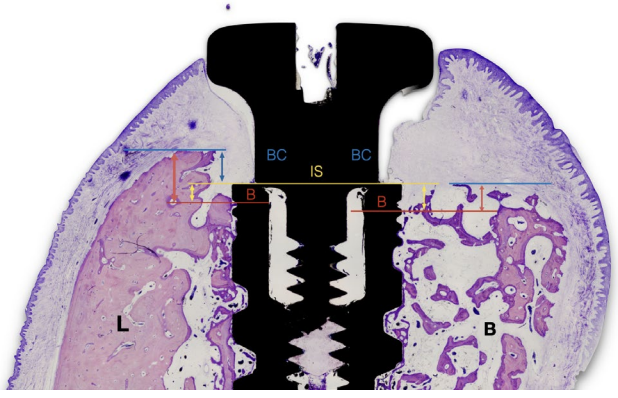

FIGURE 4 Histological landmarks: IS: Implant Shoulder. BC: Bone Crest. B: First bone–to-implant contact

3 | RESULTS

3.1 | Clinical findings

Healing of animals was uneventful in all dogs. All implants demonstrated clinical signs of adequate osseointegration and were available for histological processing.

3.2 | Histological Findings

3.2.1 | Early Healing (2 weeks)

The lingual bone crest was usually positioned coronally with respect to the implant shoulder, while the buccal bone crest was at the same level, although the first bone to implant contact was located apical to this reference. Woven bone formation represented the main histological observation within the wound chamber area in both groups,

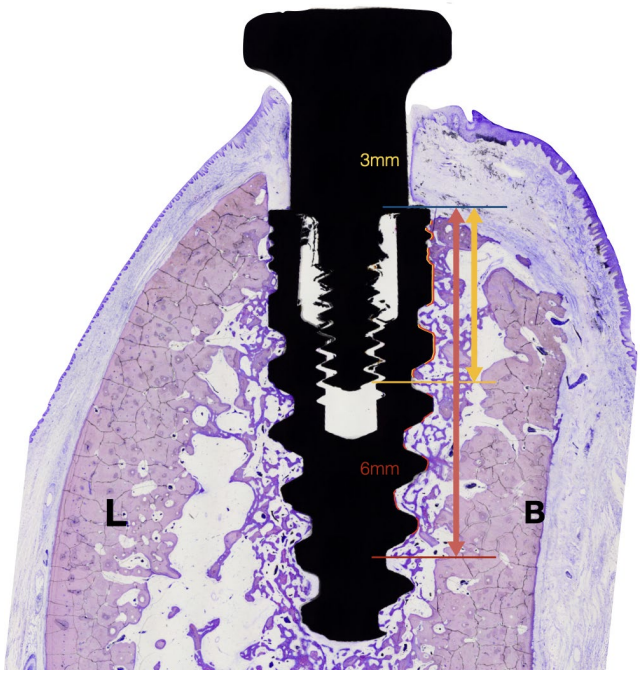

FIGURE 5 Histological bone to implant contact measurement. Coronal BIC: bone in contact with implant surface within the 3 coronal millimeters from implant shoulder. Total BIC: bone in contact with implant surface within the 6 coronal millimeters from implant shoulder

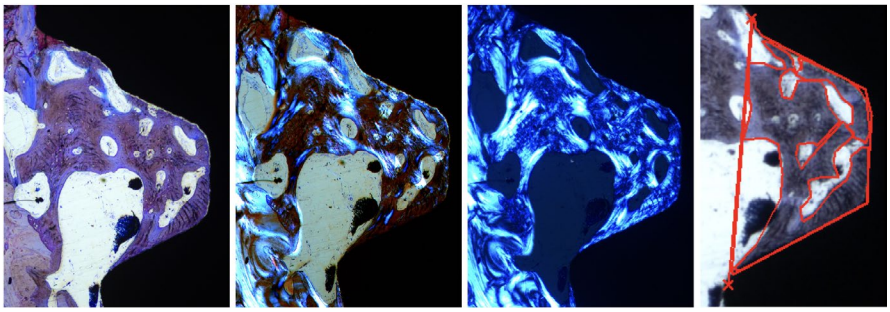

FIGURE 6 Wound chamber tissue area assessment

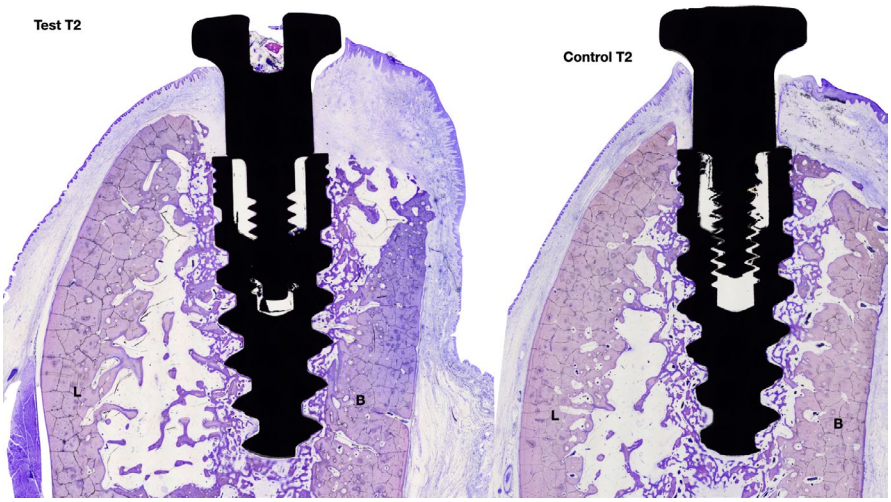

FIGURE 7 Histological section of 2-week healing implants. Note the discrepancy between crestal bone and first bone–to-implant contact (located apically with respect to implant shoulder, for both the test and control implants)

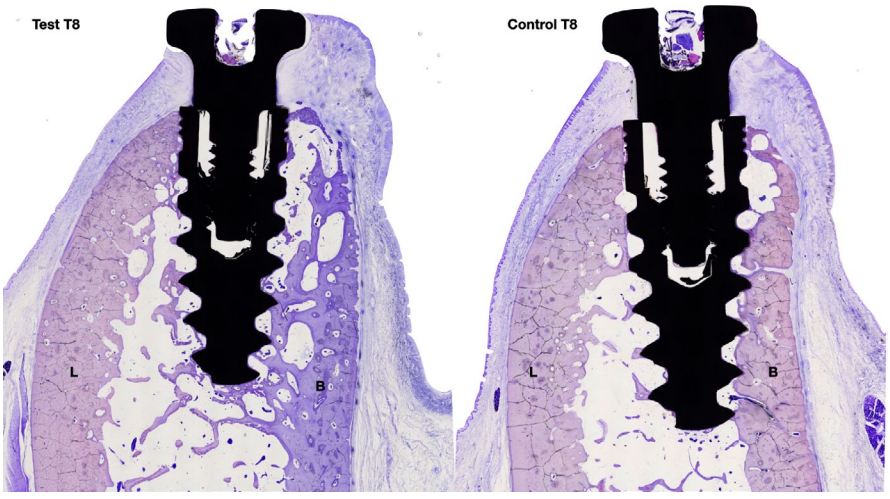

FIGURE 8 Histological section of 8-week healing implants. Note reduction in discrepancy between the apico-coronal position of the crestal bone and the first bone-to-implant contact in both implants

with this woven bone directly in contact with the implant surface. Fingerlike projections of woven bone were intercalated with non-mineralized tissue. Mature bone was observed in the thread area depicting areas of modeling and remodeling (Figure 7). No major differences were observed between the groups.

3.2.2 | Late Healing (8 weeks)

There was a slight resorption of the lingual bone crest, being positioned in close proximity to the implant shoulder. Similarly, the first bone-to-implant contact was observed in a more coronal position compared with the 2-week healing sections. Woven bone had been substituted by lamellar bone in contact with the implant surface. (Figure 8).

3.3 | Histometric results

The linear vertical measurements and BIC % are reported in (Figures 9 and 10) (Table 1). A total of 29 ground sections were available for analysis.

I-B. At two weeks, buccal and lingual average measurements showed that the first bone-to-implant contact was located

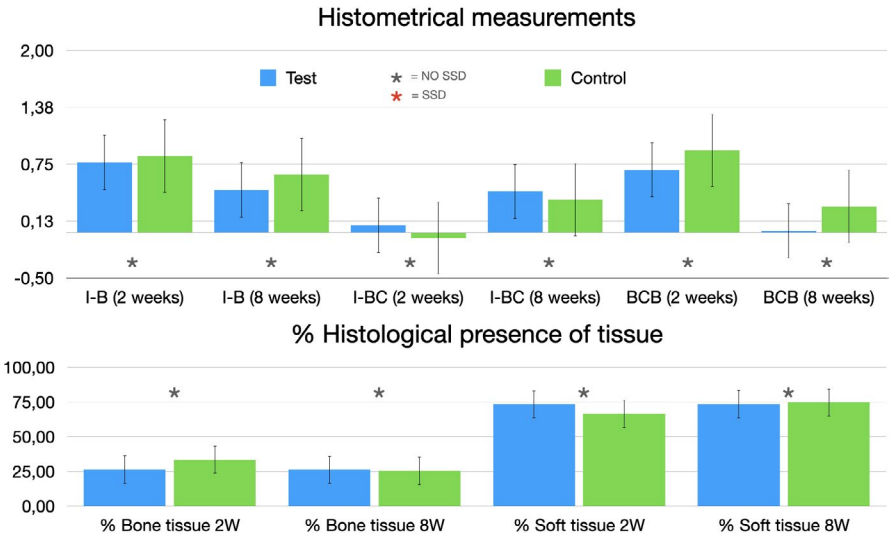

FIGURE 9 Graphical representation of linear and surface histological measurements

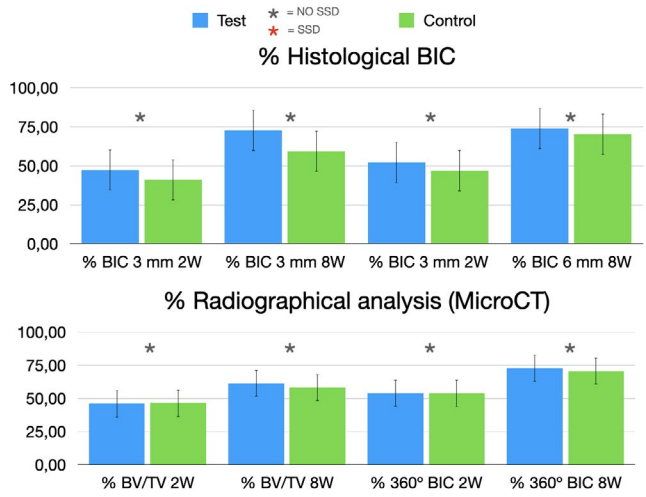

FIGURE 10 Graphical representation of histological and radiographical bone-to-implant contact and BV/TV micro-CT results

approximately 0.7–0.8 mm apical to the implant shoulder; no differences between the groups was identified. After 8 weeks of healing, the test implants showed a significant reduction in the distance between implant shoulder and first bone-to-implant contact. The first coronal level of bone contact (B) was observed at 0.47 (*SD* 0.19) and 0.64 (*SD* 0.19) for test and control groups, respectively. Differences between groups were not statistically significant.

I-Bc. Bone crest was close to implant shoulder at two weeks in both groups (test group, 0.08 mm *SD* = 0.5 versus. control group −0.06 mm *SD* = 0.28). After 8 weeks of healing, bone crest was located at 0.37 (95% CI = 0.92, 0.18) and 0.43 mm (95% CI = 0.92, 0.07) for the test and control groups, respectively. Intergroup differences were not statistically significant.

Bc-B. The distance between the bone crest and first bone-to-implant contact was reduced between 2 and 8 weeks. This reduction was as a combination of apical displacement of crestal bone and coronal growth of the first bone-to-implant contact. That reduction in distance was higher for the test (0.67 mm (95% CI = −0.16, 1.50)) compared with the control (0.62 mm (95% CI = −0.13, 1.37)). These differences between test and control were not statistically significant.

3.3.1 | Bone-to-implant contact (%BIC)

At two weeks, similar mean coronal BIC values were observed between groups (Table 2). An increase in mean BIC was observed after 8 weeks in both groups. Although a higher mean BIC value was observed for the test (74.84) when compared to control (59.46), this difference was not statistically significant.

3.3.2 | Histometrical area of tissue in the wound chambers (B and ST)

At 2 weeks, the mean area of newly formed bone was higher in control implants compared with test implants (33.48% *SD* = 12.44% versus 26.46% *SD* = 11.71, respectively) (Table 3). At eight weeks, newly formed bone area was the same between control and test implants (25.43% *SD* = 7.87% versus 26.36% *SD* = 8.50). Differences between groups were not statistically significant.

3.4 | Micro-CT results

Similar bone volume/tissue volume results were observed between test and control at 2 weeks (Table 4). Values increased in the same amount regarding test and control at 8 weeks. Around 50% of 360° radiographic bone-to-implant contact was observed in test and control at 2 weeks. A significant increase in 360° radiographic bone-to-implant contact was observed at 8 weeks in both, test and control implants (72.88% *SD* = 8.50% versus 70.75% *SD* = 7.58, respectively). Differences between groups were not statistically significant. (Figure 10).

TABLE 1 Histometrical first bone contact distance (I-B) (mean ± *SD*), bone crest distance (I-BC) (mean ± *SD*) and first bone-to-implant contact to crest distance (BCB) (mean ± *SD*) in different groups: 2-week healing, 8-week healing in both implant groups

Group	I-B 2W (mm)	I-B 8W (mm)	I-BC 2W (mm)	I-BC 8W (mm)	BCB 2W (mm)	BCB 8W (mm)
Test	0.77 ± 0.5	0.47 ± 0.19	0.08 ± 0.5	0.45 ± 0.24	0.69 ± 0.47	0.02 ± 0.20
Control	0.84 ± 0.54	0.64 ± 0.59	−0.06 ± 0.28	0.36 ± 0.34	0.90 ± 0.57	0.29 ± 0.67
Δ Test-Control	0.065	0.17	0.15	0.09	0.21	0.26
95% CI	(−0.82–0.69)	(−0.9–0.55)	(−0.39–0.68)	(−0.42–0.60)	(−1.02–0.60)	(−1.04–0.51)

Note: Means of buccal and lingual measurements are presented.

*Comparisons between groups (ANOVA test). $p < .05$. No statistically significant differences were found.

TABLE 2 Histometrical % bone-to-implant contact (BIC) in the 3 and 6 coronal mm of the implant surface in different groups: 2-week healing, 8-week healing in both implant groups

Group	BIC 3 mm 2W (%)	BIC 3 mm 8W (%)	BIC 6 mm 2W (%)	BIC 6 mm 8W (%)
Test	47.44 ± 13.81	72.84 ± 5.77	52.07 ± 14.97	73.99 ± 6.91
Control	41.11 ± 11.60	59.46 ± 14.86	46.92 ± 5.15	70.27 ± 7.94
Δ Test-Control	6.33	13.38	5.14	3.72
95% CI	(−12.34–25.00)	(−4.51–31.27)	(−8.81–19.10)	(−4.51–31.27)

Note: Means of buccal and lingual measurements are presented.

*Comparisons between groups (ANOVA test). $p < .05$. No statistically significant differences were found.

TABLE 3 Histometrical % area of mineralized tissue (B) and % area of soft tissue (ST) in different groups: 2-week healing, 8-week healing in both implant groups

Group	B 2W (%)	B 8W (%)	ST 2W (%)	ST 8W (%)
Test	26.46 ± 11.71	26.36 ± 8.50	73.54 ± 11.71	73.63 ± 8.50
Control	33.48 ± 12.44	25.43 ± 7.87	66.52 ± 12.44	74.57 ± 7.87
Δ Test-Control	7.02	0.94	7.02	0.94
95% CI	(−22.91–8.87)	(−14.29–16.17)	(−8.87–22.91)	(−16.17–14.29)

Note: Means of buccal and lingual measurements are presented.

*Comparisons between groups (ANOVA test). $p < .05$. No statistically significant differences were found.

TABLE 4 Micro-CT radiographic bone volume/tissue volume (BV/TV) and % 360° bone-to-implant contact (360 BIC) of the complete implant surface in different groups: 2-week healing, 8-week healing in both implant groups

Group	BV/TV 2W	BV/TV 8W	360 BIC 2W (%)	360 BIC 8W (%)
Test	45.99 ± 9.61	61.47 ± 12.50	53.86 ± 6.94	72.88 ± 8.50
Control	46.37 ± 7.02	58.18 ± 11.35	53.85 ± 4.81	70.75 ± 7.58
Δ Test-Control	0.37	3.30	0.01	2.12
95% CI	(−15.03–14.29)	(−11.36–17.96)	(−10.05–10.08)	(−7.94–12.19)

*Comparisons between groups (ANOVA test). $p < .05$. No statistically significant differences were found.

4 | DISCUSSION

The present experimental in vivo investigation was designed to study the histological and radiographical outcomes of a new implant surface treatment based on a monolayer of multi-phosphonate molecules, compared with a standard moderately rough implant surface, during the early and late phases of osseointegration. The novel implant surface showed a more coronal first bone-to-implant contact and a higher amount of bone-to-implant contact in the coronal third of the implant to bone interface. Furthermore, the radiographic 360 BIC percentages were superior in test group both during the early and late healing periods. At eight weeks, 360° BIC accounted for 80% approximately in the test implant, while in the control implant it was 70% (Figure 3). Similar outcomes were observed histologically. However, these differences did not reach statistical significance in any of the time evaluations when comparing the two tested implants.

This lack of statistical significance may be due to the limited sample size, which is a regular limitation in preclinical in vivo investigations. As the present study was performed according to Spanish and European animal experimentation regulations, the three "Rs" principles must be followed. The application of the reduction principle results in a sample limited to the minimum number of animals, generally between 6 and 8, which means that only strong differences will reach for statistical significance. The power obtained with eight dogs and the encountered effect between groups was 52.9%. To achieve statistical significance with eight dogs, 80% of power and 0.05 significance level, a minimal histological difference of 1.5 mm between groups should have been encountered. The mild but consistent improvements shown in the present investigation would need a much more numerous animal sample to reach statistical significance.

In spite of this lack of statistically significant differences, we may explain the consistent better results in *de novo* bone apposition on the implant surface and degree of osseointegration measured by the higher percentages in BIC by the addition of phosphonates covalently bonded to titanium that may exert an osteoconductive effect by attracting more bone-forming cells. These results coincide with a previously published experimental study using the same surface treatment in a sheep model, which reported higher removal torques and as higher bone to implant contact when compared with a control implant (von Salis-Soglio et al., 2014).

The methodology used in this investigation to evaluate the impact of implant surface modifications on the early and late stages of osseointegration has been well validated in the scientific literature. A classic osseointegration preclinical study using the wound chamber model used in this investigation reported that implants with a moderately rough surface exhibited a superior bone anchorage as compared to implants with a turned surface (Abrahamsson et al., 2004). The implant surfaces tested in the present study had both moderate micro-roughness with similar S_a values, what may explain in part the excellent results in terms of BIC and early *de novo* bone formation of the control implants.

Modern research in implant surface technology is seeking to chemically modify the implant surface to make it "bioactive," thus enhancing the bone healing dynamics immediately after implantation and facilitating early bone-to-implant contact. The addition of several ions incorporated in the implant surface, such as Ca, P, Sr, F, NaOH, and Mg, has been studied in experimental studies, reporting higher BIC percentages and removal torque values during early healing times (Albrektsson & Wennerberg, 2019). In an experimental study in mongrel dogs, Berglundh et al. observed a significant increase in BIC in the fluoride-treated implants using a similar dog experimental model (Berglundh et al., 2007). Similarly, Buser et al. (2004) reported an increase in bone-to-implant contact from 29% to 49% after two weeks and from 85% to 90% after eight weeks when implants with a moderate micro-roughness were stored in isotonic NaCl solution (Straumann SLActive® surface) in a minipig experimental model. These results were also corroborated in human histological evaluation (Lang et al., 2011). The present investigation corroborated these results also reporting a significant increase in BIC from 2 to 8 weeks, data that were confirmed with the findings in micro-CT analysis. In fact, the differences between the test and control implants in regard to the increase in bone-to-implant contact were higher at eight weeks, as compared to early healing. This difference may be due to a sustained effect of the phosphonates layer over time as a result of the covalent bonding with the titanium surface. Similar results were also reported in another experimental study evaluating the incorporation of magnesium ions to an experimental implant surface, also reporting a stronger bone response compared with control implants. The authors explained this difference by the chemical bonding promoted by Mg incorporation, in spite of a surface micro-roughness (S_a = 0.78 μm) lower than the control implants (Sul et al., 2006).

Results from this investigation should be interpreted with caution due to the inherent limitations of this experimental model. First, in experimental animal studies, the bone remodeling rates are higher than in humans and this could lead to confusion in translating the healing times and the percentages of osseointegration to the clinical situation. Also, as stated earlier, due to obvious ethical considerations, these experimental studies have limited sample sizes, which may jeopardize the proper interpretation of the results. In fact, means in bone-to-implant contact and first bone-to-implant contact are superior in test implants; however, differences did not reach statistical significance, probably due to low sample size. Another possible limitation may be related to the histological assessment, as only one plane was studied (bucco-lingual section), hence missing the structural changes occurring in the mesiodistal dimension. This limitation, however, has been partly compensated by the micro-CT analysis, which assesses BIV values 360° around the implant surface. It should also be noted that in spite of the utility of the wound chamber model to quantify the early *de novo* bone formation on the implant surface, this alteration of the implant macro-geometry does not exist in commercially available implants.

Although trends regarding bone formation seem promising toward monophosphonate implant surface, this study failed to demonstrate significant differences between phosphonate layer implants and control implants on osseointegration and position of the coronal bone attachment to the dental implant.

ACKNOWLEDGEMENTS

The authors would like to express their appreciation to Fernando Luengo and Rafael Pla for their support in the surgical procedure as well as the personnel of the Jesús Usón Minimally Invasive Surgical Center research facilities, for their invaluable support with the care of the animals. Also authors would like to acknowledge the support with the histological and micro-CT processing made by Fernando Muñoz's research team, especially to Maria Permuy.

CONFLICT OF INTEREST

The authors declare that they have no conflict of interest.

AUTHOR CONTRIBUTION

Javier Sanz-Esporrin: Data curation (lead); Formal analysis (lead); Investigation (equal); Methodology (equal); Writing-original draft

(lead). **Riccardo Di Raimondo:** Data curation (equal); Investigation (equal); Methodology (equal). **Fabio Vignoletti:** Conceptualization (equal); Investigation (equal); Methodology (equal); Supervision (lead); Writing-review & editing (equal). **Javier Nunez:** Investigation (equal); Methodology (equal); Supervision (equal); Writing-review & editing (equal). **Fernando MuÑoz:** Data curation (supporting); Resources (equal); Visualization (equal); Writing-review & editing (equal). **Mariano Sanz:** Conceptualization (lead); Funding acquisition (lead); Investigation (equal); Methodology (equal); Project administration (lead); Resources (equal); Supervision (lead); Visualization (lead); Writing-review & editing (lead).

DATA AVAILABILITY STATEMENT

The data that support the findings of this study are available from the corresponding author upon reasonable request.

ORCID

Javier Sanz-Esporrin https://orcid.org/0000-0003-0859-3149
Fabio Vignoletti https://orcid.org/0000-0002-4574-3671
Fernando Muñoz https://orcid.org/0000-0002-4130-1526
Mariano Sanz https://orcid.org/0000-0002-6293-5755

REFERENCES

Abrahamsson, I., Berglundh, T., Linder, E., Lang, N. P., & Lindhe, J. (2004). Early bone formation adjacent to rough and turned endosseous implant surfaces. An experimental study in the dog. *Clinical Oral Implants Research*, *15*(4), 381–392. https://doi.org/10.1111/j.1600-0501.2004.01082.x

Abrahamsson, I., Linder, E., Larsson, L., & Berglundh, T. (2013). Deposition of nanometer scaled calcium-phosphate crystals to implants with a dual acid-etched surface does not improve early tissue integration. *Clinical Oral Implants Research*, *24*(1), 57–62. https://doi.org/10.1111/j.1600-0501.2012.02424.x

Albrektsson, T., Branemark, P. I., Hansson, H. A., & Lindstrom, J. (1981). Osseointegrated titanium implants. Requirements for ensuring a long-lasting, direct bone-to-implant anchorage in man. *Acta Orthopaedica Scandinavica*, *52*(2), 155–170. https://doi.org/10.3109/17453678108991776

Albrektsson, T., Sennerby, L., & Wennerberg, A. (2008). State of the art of oral implants. *Periodontology 2000*, *47*(1), 15–26. https://doi.org/10.1111/j.1600-0757.2007.00247.x

Albrektsson, T., & Wennerberg, A. (2019). On osseointegration in relation to implant surfaces. *Clinical Implant Dentistry and Related Research*, *21*(Suppl 1), 4–7. https://doi.org/10.1111/cid.12742

Berglundh, T., Abrahamsson, I., Albouy, J. P., & Lindhe, J. (2007). Bone healing at implants with a fluoride-modified surface: An experimental study in dogs. *Clinical Oral Implants Research*, *18*(2), 147–152. https://doi.org/10.1111/j.1600-0501.2006.01309.x

Berglundh, T., Abrahamsson, I., Lang, N. P., & Lindhe, J. (2003). *De novo* alveolar bone formation adjacent to endosseous implants. *Clinical Oral Implants Research*, *14*(3), 251–262. https://doi.org/10.1034/j.1600-0501.2003.00972.x

Berglundh, T., Lindhe, J., Jonsson, K., & Ericsson, I. (1994). The topography of the vascular systems in the periodontal and peri-implant tissues in the dog. *Journal of Clinical Periodontology*, *21*(3), 189–193. https://doi.org/10.1111/j.1600-051x.1994.tb00302.x

Branemark, P. I., Adell, R., Breine, U., Hansson, B. O., Lindstrom, J., & Ohlsson, A. (1969). Intra-osseous anchorage of dental prostheses. I. Experimental studies. *Scandinavian Journal of Plastic and Reconstructive Surgery*, *3*(2), 81–100. https://doi.org/10.3109/02844316909036699

Branemark, P. I., Hansson, B. O., Adell, R., Breine, U., Lindstrom, J., Hallen, O., & Ohman, A. (1977). Osseointegrated implants in the treatment of the edentulous jaw. Experience from a 10-year period. *Scandinavian Journal of Plastic and Reconstructive Surgery Supplementum*, *16*, 1–132.

Buser, D., Broggini, N., Wieland, M., Schenk, R. K., Denzer, A. J., Cochran, D. L., Hoffmann, B., Lussi, A., & Steinemann, S. G. (2004). Enhanced bone apposition to a chemically modified SLA titanium surface. *Journal of Dental Research*, *83*(7), 529–533. https://doi.org/10.1177/154405910408300704

Buser, D., Schenk, R. K., Steinemann, S., Fiorellini, J. P., Fox, C. H., & Stich, H. (1991). Influence of surface characteristics on bone integration of titanium implants. A histomorphometric study in miniature pigs. *Journal of Biomedical Materials Research*, *25*(7), 889–902. https://doi.org/10.1002/jbm.820250708

Cochran, D. L. (1999). A comparison of endosseous dental implant surfaces. *Journal of Periodontology*, *70*(12), 1523–1539. https://doi.org/10.1902/jop.1999.70.12.1523

Donath, K., & Breuner, G. (1982). A method for the study of undecalcified bones and teeth with attached soft tissues. The Sage-Schliff (sawing and grinding) technique. *Journal of Oral Pathology and Medicine*, *11*(4), 318–326. https://doi.org/10.1111/j.1600-0714.1982.tb00172.x

Ellingsen, J. E., Johansson, C. B., Wennerberg, A., & Holmen, A. (2004). Improved retention and bone-tolmplant contact with fluoride-modified titanium implants. *The International Journal of Oral & Maxillofacial Implants*, *19*(5), 659–666.

Jeno, L., & Geza, L. (1975). A simple differential staining method for semithin sections of ossifying cartilage and bone tissues embedded in epoxy resin. *Mikroskopie*, *31*(1–2), 1–4.

Junker, R., Dimakis, A., Thoneick, M., & Jansen, J. A. (2009). Effects of implant surface coatings and composition on bone integration: A systematic review. *Clinical Oral Implants Research*, *20*(Suppl 4), 185–206. https://doi.org/10.1111/j.1600-0501.2009.01777.x

Lang, N. P., Salvi, G. E., Huynh-Ba, G., Ivanovski, S., Donos, N., & Bosshardt, D. D. (2011). Early osseointegration to hydrophilic and hydrophobic implant surfaces in humans. *Clinical Oral Implants Research*, *22*(4), 349–356. https://doi.org/10.1111/j.1600-0501.2011.02172.x

Lazzara, R. J., Porter, S. S., Testori, T., Galante, J., & Zetterqvist, L. (1998). A prospective multicenter study evaluating loading of osseotite implants two months after placement: One-year results. *Journal of Esthetic and Restorative Dentistry*, *10*(6), 280–289. https://doi.org/10.1111/j.1708-8240.1998.tb00505.x

Sul, Y. T., Johansson, C., & Albrektsson, T. (2006). Which surface properties enhance bone response to implants? Comparison of oxidized magnesium, TiUnite, and Osseotite implant surfaces. *The International Journal of Prosthodontics*, *19*(4), 319–328.

van Oirschot, B. A., Bronkhorst, E. M., van den Beucken, J. J., Meijer, G. J., Jansen, J. A., & Junker, R. (2013). Long-term survival of calcium phosphate-coated dental implants: A meta-analytical approach to the clinical literature. *Clinical Oral Implants Research*, *24*(4), 355–362. https://doi.org/10.1111/clr.12063

Vignoletti, F., Sanz-Esporrin, J., Sanz-Martin, I., Nunez, J., Luengo, F., & Sanz, M. (2019). Ridge alterations after implant placement in fresh extraction sockets or in healed crests: An experimental in vivo investigation. *Clinical Oral Implants Research*, *30*(4), 353–363. https://doi.org/10.1111/clr.13421

Viornery, C., Guenther, H. L., Aronsson, B. O., Pechy, P., Descouts, P., & Gratzel, M. (2002). Osteoblast culture on polished titanium disks modified with phosphonic acids. *Journal of Biomedical Materials Research*, *62*(1), 149–155. https://doi.org/10.1002/jbm.10205

von Salis-Soglio, M., Stübinger, S., Sidler, M., Klein, K., Ferguson, S., Kämpf, K., Zlinszky, K., Buchini, S., Curno, R., Péchy, P., Aronsson, B.-O., & von Rechenberg, B. (2014). A novel multi-phosphonate surface treatment of titanium dental implants: A study in sheep. *Journal of*

Functional Biomaterials, *5*(3), 135–157. https://doi.org/10.3390/jfb5030135

Wennerberg, A., Albrektsson, T., Andersson, B., & Krol, J. J. (1995). A histomorphometric and removal torque study of screw-shaped titanium implants with three different surface topographies. *Clinical Oral Implants Research*, *6*(1), 24–30. https://doi.org/10.1034/j.1600-0501.1995.060103.x

Wheeler, S. L. (1996). Eight-year clinical retrospective study of titanium plasma-sprayed and hydroxyapatite-coated cylinder implants. *The International Journal of Oral & Maxillofacial Implants*, *11*(3), 340–350.

SUPPORTING INFORMATION

Additional supporting information may be found online in the Supporting Information section.

How to cite this article: Sanz-Esporrin, J., Di Raimondo, R., Vignoletti, F., Núñez, J., Muñoz, F., & Sanz, M. (2021). *De novo* bone formation around implants with a surface based on a monolayer of multi-phosphonate molecules. An experimental in vivo investigation. *Clinical Oral Implants Research*, 32, 1085–1096. https://doi.org/10.1111/clr.13803